Digest Journal of Nanomaterials and Biostructures Vol. 13, No. 1, January - March 2018, p. 163 - 176

COMPARISON OF MULTIPLE LINEAR REGRESSION ANALYSIS AND ARTIFICIAL NEURAL NETWORK APPROACHES IN THE ESTIMATION OF MONTE CARLO MEAN GLANDULAR DOSE CALCULATIONS OF MAMMOGRAPHY

T. T. ERGUZEL[a], H. O. TEKIN[bc*], T. MANICI[c], E. E. ALTUNSOY[cd], N. TARHAN[e]

[a]*Uskudar University, Department of Software Engineering, Istanbul, Turkey*
[b]*Uskudar University, Department of Radiotherapy, Istanbul, Turkey*
[c]*Uskudar University, Medical Radiation Research Center (USMERA), Istanbul, Turkey*
[d]*Uskudar University, Department of Medical Imaging, Istanbul, Turkey*
[e]*Uskudar University, Department of Psychology, Istanbul, Turkey*

Mammography is an x-ray based breast imaging process which uses radiological method as a non-invasive way for the diagnosis of breast diseases common among woman subjects. A breast screening operation employs mammography in the early recognition of abnormalities in breast construction such as micro-calcifications, which could develop a breast carcinoma. On the other hand, breast dosimetry is an indispensable issue on behalf of patient radiation safety and evaluation of potential risks from medical radiation. In this study, we first aimed to investigate capabilities of Monte Carlo N-Particle eXtended (MCNPX) code for calculations of Mean Glandular Dose (MGD) in a mathematical breast phantom during mammography screening. MGD values were investigated by using MCNPX (version 2.4.0) Monte Carlo code. A mathematical breast phantom has been modeled in an average shape by defining the dimensions x, y and z. The breast model has been considered as semi-elliptical cylindrical geometry in different thicknesses as cranio-caudal projection. Afterwards, x-ray spectra from W/Rh target-filter combination has been obtained and defined as a spectrum into source definition in MCNPX input file. Following the Monte Carlo calculations process, a linear, multiple linear regression analysis (MLRA), and a nonlinear, artificial neural network (ANN), approach was employed in order to put forward an alternative predictive model. Finally, the performance comparison of the aforementioned models were expressed in terms of five accuracy indices, Mean Absolute Error (MAE), Mean Absolute Percentage Error (MAPE), Root Mean Square Error (RMSE), Normalized Root Mean Square Error (NRMSE) and R^2 coefficient of determination. The results underlined that both of the models perform quite satisfactorily and MGD values are strongly correlated with three independent variables which are breast thickness, X-ray spectra and glandular-adipose rate.

(Received October 17, 2017; Accepted January 25, 2018)

Keywords: Mammography, Mean glandular dose prediction, Monte Carlo, Artificial neural network, Multiple linear regression analysis

1. Introduction

It is agreed that, the use of X-rays for medical operations is the major artificial source for exposure of population to ionizing radiation. So far, x-rays has been used in various medical applications to serve as a tool for diagnostic and therapeutic aims. Mammography is an x-ray based imaging modality which uses radiological process as a non-invasive technique for the diagnosis of breast diseases in women. Being a valuable breast screening process, mammography highlights the early recognition of anatomic

*Corresponding author: huseyinozan.tekin@uskudar.edu.tr

abnormalities observed in breast structure such as micro-calcifications that may cause breast carcinoma. On the other hand, breast dosimetry is a significant issue on behalf of patient radiation safety and assessment of potential risks from radiation. Proper dosimetry of the dose magnitude absorbed by breast during the mammography examination is a topic to be focused on and was studied for long [1-7]. The dose magnitude to the breast tissue depends on some quantities such as target/filter spectra, breast composition, thickness and shape of breast and energy value. The glandular tissue of breast known as a radiosensitive organ which is primary evaluated in terms of breast dosimetry and can be adversely affected from ionizing radiation during the mammography examinations [8]. Therefore, calculating the mean glandular dose (MGD) in the breast tissue is the quite significant for assessment of average dose to the breast. MGD is a magnitude that gives the average dose absorbed in the breast. Mammography uses low-dose protocols in accordance with ALARA (As Low As Reasonably Achievable) principle. However, it is not possible to measure the average dose directly since it depends on the kVp, target/filter combination, breast composition and thickness of breast parameters. So far, the magnitude of MGD of breast have been calculated using Monte Carlo in various studies [9-11]. The MGD dataset was gathered using MCNPX (version 2.4.0) Monte Carlo code for W/Rh anode-filter combinations that used in latest mammography devices. Firstly, X-ray spectra has been obtained W/Rh anode-filter in the tube voltage from 26kV to 32 kV with 2 kV spacings and obtained x-ray spectra has been defined as energy source for the MGD calculations. The calculations have been repeated for different glandular-adipose breast compositions (0% to 100% glandular with 10% intervals) and compressed breast thicknesses from 2 to 12 cm with 1 cm spacing respectively. We defined different mathematical breast phantoms for each glandular-adipose compositions and different breast thickness by considering the compressed cranio-caudal projection. The modeled mathematical breast phantom is depicted in figure 1.

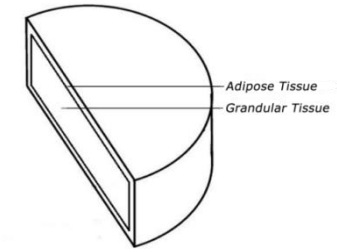

Fig. 1. The schematic representation of modeled breast phantom

Following the first step, we calculated MGD (mGy) values according to simulation geometry that is given in figure 2. As it can be seen in Fig. 2, accelerated electron beam interact with W anode material and x-ray beam has been produced.

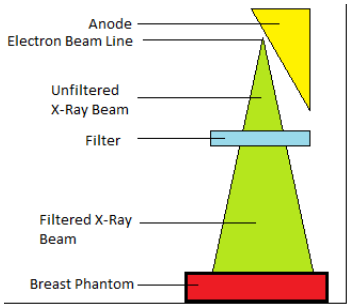

Fig. 2. Total simulation geometry

Lately, computer-based methods such as artificial neural networks (ANNs) and multiple linear regression analysis (MLRA) have attracted some attentions to be replaced with high-cost experimental studies. In recent studies, surrogate methods are being widely used to substitute for numerical models or experiments including the multiple linear regressions [12, 13], the artificial neural networks [14-16] to estimate the MGD. These surrogate methods can construct the relationship between the input variables and the output values while decreasing the computational time. Because of the lack of the studies investigating the applicability of those methods to estimate the MGD value, our study focused on predicting MGD values addressing MLRA and ANN approaches. Apart from former studies, MCNPX simulations on mean glandular dose investigates extensive breast thickness ranging from 2cm to 12cm. Besides, comparing a nonlinear and a linear approach is a promising field of study with its highly valuable contribution to predictive approaches. Therefore, the application of MLRA and ANN methods studied in our research is a valuable perspective to be considered for similar predictive studies.

2. Material and Methods

In this research, assessment of MLRA and ANN on MGD estimation in mammography examination has been studied. For this aim, Monte Carlo simulation of MGD dose calculations for different mathematical breast phantoms have been studied first. In order to predict the MC dose calculations a linear, MLRA, and a nonlinear approach, ANN, have been applied respectively.

2.1. Monte Carlo Simulation and Breast Phantom

MCNPX (version 2.4.0) Monte Carlo code has been used for investigations on MGD calculations. MCNPX is a radiation transport code for modeling the interaction of radiation with materials and also tracks all particles at wide range energies. MCNPX is fully three-dimensional and it utilizes extended nuclear cross section libraries and uses physics models for particle types. [17]. Various simulation studies on medical applications and for other aims by using MCNPX Monte Carlo code are found in literature [18-22].

Apart from the general approaches to medical applications, MCNPX is also significantly useful and effective tool for mammography studies [23]. As a first step of simulation geometry, MCNPX simulation parameters such as cell definitions, surface definitions, material definition and position of each tool, definitions and features of sources have been defined in input file according to their properties. The geometrical forms and physical parameters of mammography device have been defined. The schematic view of total simulation setup shown in figure 2. As it can be clearly seen in figure, an x-ray source (W target / 26-32 kV) positioned at up of the filtering materials with the focal

spot of 0.3 mm. Afterwards, x-ray spectra from W/Rh target-filter combination has been obtained and defined as a spectrum into energy source definition in MCNPX input file. To acquire energy deposition in a specific volume, F6 tally mesh has been used to obtain the absorbed energy amount in breast tissue.

In this research, the spectra of W-Rh target-filter combination were generated at tube voltages of 26 kV, 28 kV, 30 kV and 32 kV, respectively. The simulation results were completed by using Intel® Core ™ i7 CPU 2.80 GHz computer. In MCNPX simulation, 10^6 particles have been traced. During the simulation study, the error rate has been observed less than %1 in output file. The obtained x-ray spectra was defined as energy source for the next step of simulation. The mathematical breast phantom with 8 cm radius in cranio-caudal projection has been located in below of x-ray beam. As it can be seen in figure 1, glandular tissue of mathematical breast phantom has been surrounded with 0.5 cm adipose tissue. The elemental mass fractions and densities of different glandular-adipose rate mathematical breast samples [24] have been defined. Eventually, Mean Glandular Dose values have been calculated by using the portion of the absorbed energy value in the glandular tissue of the mathematical breast phantom G(E) and absorbed dose distribution D(E) as the output of F6 tally in breast tissue [25].

2.2. Multiple Linear Regression Analysis

Given the dependent variable Y and the set of p predictor variables $X_1 \ldots X_p$, the multiple linear regression model assumes that the mean of Y determines the values of the predictor variables in a linear combination as given in equation 1.

$$Y = \beta_0 + \beta_1 X_1 + \cdots \beta_p X_p + e \tag{1}$$

MLRA is a statistical approach that is used to determine a relationship between a dependent variable and a number of independent variables. In fact, the dependent variable is a linear function of more than one independent variable. Linear regressions are mostly fitted using least squares approach. MLR model is a classic technique providing several advantages: simplicity, interpretability, possibility of being adjusted over the transformations of the variables, and the performing of reasoning, supposing the hypothesis of normality, homoscedasticity and correlation between the error ε and the predictor parameters. In this study, IBM SPSS Statistics Version 24 was used to generate the MLR model. MLR models do not require any additional configuration for the parameters by means of validation process, thus they were adjusted on the basis of the conjunction of both validation and training sets, being later applied to the test dataset [26]. Basically, the linear regression is divided into two categorizations of simple and Multiple Linear Regression. If the aim is to estimate the linear correlation between one dependent and one independent variable, the model is assumed as the simple linear regression (SLR). On the other hand, if the aim is to predict the linear correlation between two or more independent variables and still one dependent variable, the model is called as MLR. It is worth mentioning that the MLR is the most common form of linear regression analysis and every value of the independent variable is associated with a value of dependent variable. Normally, MLR models estimate the level of correlation between one response variable (dependent variable) from two or more predictors (Independent variable). In this analysis, the correlation coefficient, R^2, describes the proportion or percentage of variance in the dependent variable explained by the variance in the independent variables together which sometimes called the predictor variables. An R^2 of "1.00" indicates that 100% of the variation in the dependent variable is explained by the independent variables. Conversely, an R^2 of "0.0" indicates the absence of variation in the dependent variable due to the independent variables. It should be emphasized that the MLR explores a correlation in terms of a straight line that best predicts all the individual data points containing both target and output variables [27]. MLR is developed based on two assumptions: (i) the explanatory variables must be independent, and (ii) the dependent variable must be normally distributed with zero mean and constant variance. In regression equations the collinearity between the explanatory variables can

lead to some drawbacks due to the fact that high correlations between predictor variables could cause some difficulty for a correct analysis [28]. Some methods such as enter, stepwise, backward elimination and forward methods can be applied to valid regression coefficients. In this study, stepwise method was applied to determine the significant regression coefficients. The application of these methods leads to the exclusion of explanatory independent variables which have less correlation with the output variable [29].

2.3. Artificial Neural Network

Artificial neural network is a data processing system inspired by the form of human brain. ANN is basically made of artificial neurons which are described as highly interconnected processing cells to solve a specific modelling problem. ANN is a powerful modeling tool compared to the statistical or numerical methods [30], and i widely used for many engineering applications such as prediction, optimization, classification and pattern recognition [31] processes. Artificial neurons in the ANN are arranged in different layers of the network and each layer is connected following a junction point called activation function. Each network comprises an input layer, an output layer and one or more hidden layers [32]. The neurons in the networks are interconnected using weight factors (w_{ij}). A neuron (j) in a given layer receives information (x_i) from the inputs all the neurons in the preceding layer as given in figure 3. It sums up information (net_j) weighted by factors and the bias of the layer (θ_j) Later it transmits output values (y_j) applying an activation function f() to net_j, to all neurons of the next layer [33].

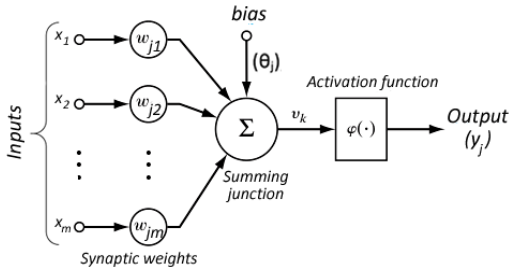

Fig. 3 Artificial neuron structure

ANN has been inspired by biological neural networks; it consists of simple neurons and connections that process information in order to find a relationship between inputs and outputs. The most common ANN architecture used by hydrologist is the Multilayer Perceptrons (MLP) which is a feedforward network that consists of three layers of neurons, the input layer, the hidden layers and the output layer. The number of input and output neurons is based on the number of input and output data; The input layer only serves as receiving the input data for further processing in the network. The hidden layers are a very important part in an MLP since they provide the nonlinearity between the input and output sets. More complex problems can be solved by increasing the number of hidden layers or the hidden neurons in the hidden layers. The output neuron is the desired output of the model. The process of developing an ANN model is to find (a) suitable input dataset, (b) determine the number of hidden layers and neurons, and (c) training, validating and testing the network. The network could be expressed as given in equation 2.

$$Y_t = f_2\left[\sum_{j=1}^{J} W_j f_1\left(\sum_{i=1}^{I} W_i X_i\right)\right] \quad (2)$$

where Y_t is the output, x_i is the input vector, w_i and w_j are the weights between neurons of the input and hidden layer and between hidden layer and output while f_1 and f_2 are the activation functions for the hidden layer and output layer respectively. According to a recent study, sigmoidal-type transfer functions are recommended for the hidden and linear

transfer functions are proposed for output layers. In this study f_1 is considered *hyperbolic tangent sigmoid* function which is a nonlinear function and f_2 is considered the linear *purelin* function defined as given in equation 3 and 4 respectively [34].

$$f_1(x) = \frac{1}{(1+\exp(-2x))} - 1 \tag{3}$$

$$f_2(x) = x \tag{4}$$

The ANN models were trained based on Levenberg–Marquardt algorithm; number of hidden neurons was chosen based on trial and error process. In ANN modelling there is always the probability of generating an over-fitted model. In order to avoid this problem early stopping technique is applied in this study while training and validating the models. Through this approach, the network stops the training when the error over the validation dataset starts to increase while the error over training dataset is still decreasing. The network avoids overfitting in this way [35]. Here, the activation function demonstrates the relationship between the inputs and outputs of a node and a network. Literaly, it indicates a degree of nonlinearity that is applicable for the most ANN modeling approaches. In our study, sigmoid function is used for the first layer and purelin function for the output layer.

2.3.1 Neural Network Training

The neural network training is an unconstrained nonlinear minimization problem in which weights of a model are iteratively updated to minimize error between the target and the model output considering the input patterns. Various training methods exist to generate an optimal ANN model. But, there is still no training algorithm ensuring the global optimal solution for a general nonlinear optimization problem in a reasonable amount of time [36, 37]. Recent studies highlight the performance of back-propagation (BP) training algorithm methods used for multi-layered feed-forward networks that is essentially a gradient steepest descent method. For the gradient descent algorithm, a step size, which is called the learning rate in ANN structure, must be defined. The learning rate is another parameter for back-propagation learning algorithm since it determines the magnitude of weight changes for each epoch. As to the number of hidden layers and the number of neurons used in the layers, there is no general rule to determine the numbers. It is also a trial and error process to identify the optimal and general network. The number of neurons is to be decided properly to predict the desired parameters correctly. Most researchers have conducted many studies to determine the appropriate number of neurons, and have presented different approaches. The general idea underlines that the upper bound for the number of neurons in the hidden layer is to be limited to twice the number of inputs plus one [38]. In this study, the ANN toolbox in MATLAB is used to compute the predicted outputs. In this regard, a 3-layered feed-forward network trained by the various training functions and is employed. LMBP is assumed as the fastest back-propagation algorithm and highly recommended while it requires more memory than other algorithms [39]. The gradient descent with a momentum backpropagation algorithm (learngdm) was used as the adaption learning function. A nonlinear hyperbolic tangent sigmoid and log-sigmoid functions for the hidden layer and a linear activation functions are used for the output layer. General structure of the generated model is given in figure 4 [40].

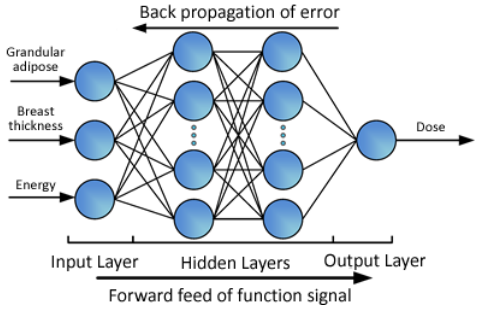

Fig. 4 Neural Network architecture of the designed model

2.4. Performance Evaluation for MLRA and ANN Models

Based on training data, prediction accuracy which is the most important measure of performance can be estimated [41]. The difference between the actual (target) and the predicted value is its forecasting error which represents the accuracy measure. In order to evaluate the performance of the applied models in this study, five accuracy measures have been calculated. To assess the validity of the prediction models, mean absolute error (MAE), the mean absolute percentage error(MAPE), the root mean square error (RMSE), Normalized Root Mean Square Error (NRMSE) and coefficients of determination (R^2) were used. The MAE, MAPE, RMSE, NRMSE and R^2 values were calculated using equations 5-9, respectively. The models providing the best prediction values were chosen as the prediction models. The MAE value was computed using equation 5.

$$MAE = \frac{1}{N}\sum_{i=1}^{N}(|t_i - td_i|) \tag{5}$$

where t_i is the measured value of the experimental samples, t_{di} is the predicted value, and N is the total number of samples. if MAE approaches *"0"*, it is an indication of the model's high accuracy.

$$MAPE = \frac{1}{N}\left(\sum_{i=1}^{N}\left[\left[\frac{t_i - td_i}{t_i}\right]\right]\right) * 100 \tag{6}$$

The closer MAPE value is to *"0"*, the better the performance of the model is.

$$RMSE = \sqrt{\frac{1}{N}\sum_{i=1}^{N}(t_i - td_i)^2} \tag{7}$$

RMSE values close to *"0"* also denote good performance on the part of the model.

$$RMSE = \sqrt{\frac{\sum_{i=1}^{n}\left(P_{sim}^{i} - P_{obs}^{i}\right)^2}{\sum_{i=1}^{n}(P_{obs}^{i})^2}} \tag{8}$$

where P_{sim} is the simulated dose value and P_{obs} is the actual dose value of the mean.
NRMSE value close to one indicates a poor model performance, whereas value close to *"0"* shows a good model performance.

$$R^2 = 1 - \frac{\sum_{i=1}^{N}(t_i - td_i)^2}{\sum_{i=1}^{N}(t_i - \bar{t})^2} \tag{9}$$

where, $\bar{t}$ is the average of predicted values. Coefficients of *"1"* or almost *"1"* indicate that the model can yield reliable results [42].

3. Model Assessment

3.1. Verifying the performance of ANN in predicting the mean glandular dose

In order to reveal the performance of ANN models and MLRA model, five aforementioned accuracy indices were considered. First, prior to the ANN model determinig process, tansig, logsig activation functions for hidden layer, Levenberg-Marquardt (trainlm), bayesian regularization (trainbr), gradient descent with adaptive learning rate backpropagation (traingda) training functions and three network structures with various number of neurons for input, hidden and output layers were created. The number of neurons for each layer is assigned as 3-10-1, 3-15-1, 3-20-1 respectively. In order to overcome the overfitting problem, early stopping method was used to in all of the designed networks. With this approach, the available data were divided into three subsets, training, validation and test set. Training set was used for updating the network weights and biases throughout the modelling process while the second subset, validation set is used to monitor the training process for specifying the process stopping point. It was decided that training will automatically stop when generalization stops improving, as indicated by an increase in the mean square error (MSE) of the validation samples. Afterward, when the network begins to over-fit the data, the error in the validation set begins to rise, while the error in training set is still decreasing. As given in figure 5, when the validation error increases for 6 epochs following the 28th epoch where the best validation performance is obtained, the training process is stopped and the weight, bias values at the minimum of the validation error are returned and reported [42].

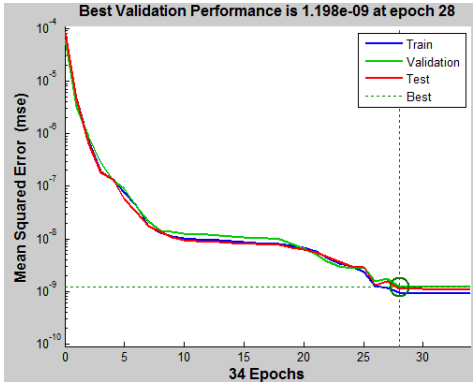

Fig. 5. The output of MSE variation throughout the ANN model generating process

Considering the various network structures and evaluation methods, 6 feed-forward backpropagation network models were created. The performance of each model is given in table 1. In order to introduce the best ANN structure to predict the mean dose, various structures of ANN with three layers (input, hidden and output layer) are designed and assessed based on five accuracy indices. According to table 1, the optimal network has TrainBR training algorithm and Logsig transfer function with 15 neurons in hidden layer (3–15–1). On the other hand, the performance of the first model using TrainLM is quite satisfactory compared to the fifth model. But, since the number of iterations therefore the time spent to generate the model is quite different for each, the number of iterations is considered as the discriminative feature to select the outperforming model. Recent studies

underlined that TrainLM is the fastest back-propagation algorithm and is highly recommended despite the fact that it requires more memory than other algorithms [39]. Therefore, the first model using TrainLM with 10 neurons in the hidden layer is selected as the optimal dose predicting model.

Table 1. The specifications and performance measures of six different ANN structure

Activation Function	Model ID	Training Function	Network Structure	Number of iterations	Training Set					Test Set				
					R	*MAE*	*MAPE (%)*	*RMSE*	*NRMSE*	*R*	*MAE*	*MAPE (%)*	*RMSE*	*NRMSE*
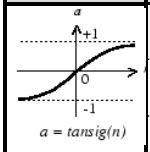 *a = tansig(n)*	*1*	TrainLM	3-10-1	38	0,999	0,00001	0,0046	0,00006	0,00349	0.999	0,00003	0,0057	0,00098	0,05371
	2	TrainBR	3-15-1	893	0,999	0,00002	0,0051	0,00000	0,00013	0.999	0,00031	0,0067	0,00001	0,00076
	3	TrainGDA	3-20-1	288	0,962	0,00089	0,0896	0,00202	0,11079	0,96	0,00107	0,0967	0,00953	0,52380
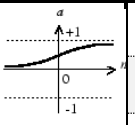 *a = logsig(n)*	4	TrainLM	3-10-1	54	0,999	0,00007	0,0057	0,00010	0,00532	0.999	0,00010	0,0064	0,00011	0,00611
	5	TrainBR	3-15-1	937	1	0,00001	0,0035	0,00001	0,00082	1	0,00001	0,0046	0,00015	0,00827
	6	TrainGDA	3-20-1	427	0,967	0,00118	0,0875	0,00121	0,06628	0,95	0,00318	0,1007	0,01206	0,66283

Considering the results given above, regression curve for training, validation and test dataset is plotted for the first model with id 1, as given in Fig. 6. The test results underline that pearson correlation coefficient is 0.999 and the output function for the test dataset is expressed as *0,93*target+0.0091* that represents a high correlation between the target value and model output.

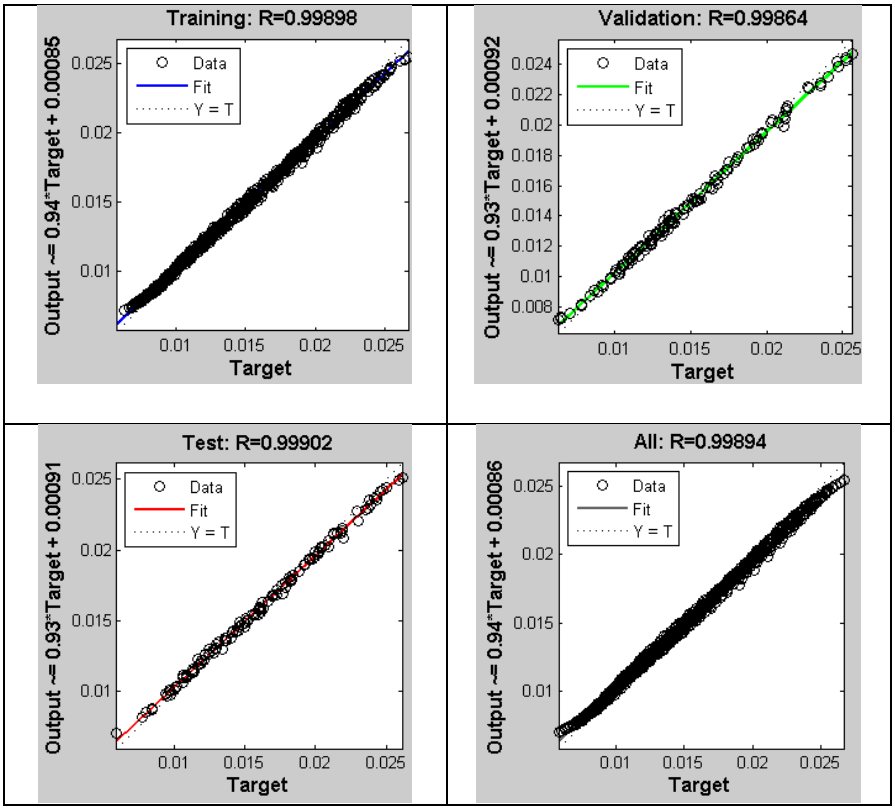

Fig. 6 The output of MSE variation throughout the ANN model generating process

3.2 Verifying the performance of MLRA in predicting the Mean Glandular Dose

For a better selection of the independent variable set it is crucial to select the optimal regression model. To achieve this, a stepwise regression, basically a semi-automated tool of building a regression model by successively including or excluding the independent variables based solely on the t-statistics of their estimated coefficients has been applied by means of the forward selection, was implemented in IBM SPSS Statistics Version 24. In order to validate the model, the validation process that involves an initial stepwise regression on the full dataset and a second stepwise regression on a random sample of 75% of the cases were performed. The resulting equations of the full training and partial training models were compared in terms of the independent variables included in the models.

Table 2. Stepwise Regression Results of Predictors

Model	R	R		R-square		Std. Error of the Estimate (75% of dataset)	Validation Check
	Training Set (whole dataset)	Training Set (75% of dataset)	Validation Set (25% of dataset)	Training Set (75% of dataset)	Validation Set (25% of dataset)		
1	0,865[a]	0,851[a]	-	0,724	-	0,00250	-
2	0,954[b]	0,951[b]	-	0,904	-	0,00150	-
3	0,988[c]	0,987[c]	0,989	***0,974***	***0,978***	0,00078	0,071

a. Predictors: (Constant), breast thickness (cm)
b. Predictors: (Constant), breast thickness (cm), X-ray spectra (kV)
c. Predictors: (Constant), breast thickness (cm), X-ray spectra (kV), Glandular Adipose

The results given in table 2 underlines the fact that the third MLR model which adds all independent variables, breast thickness, X-ray spectra and glandular adipose, into the models outperforms compared to two former models considering both the standard error of the estimate and R-square value. It was also checked whether or not there is a significant decrease in the R-squares between the training group (75% of the cases) and the validation group (25% of the cases). Since the R-square value of the validation group is less than 2% compared to the R-square value of training group, the model is validated. Following the stepwise regression, the standardized, unstandardized coefficients and the significance parameters are calculated for each model as given in table 3 in order to focus on the "statistically significance" scale, that represents the contribution to the model prediction performance.

Table 3. Stepwise Models and Model Coefficients

Model		**Unstandardized Coefficients**		**Standardized Coefficients**	**t**	**Significance**
		Beta	**Std. Error**	**Beta**		
1	(Constant)	0,024	0,000	-	75,294	0,000
	Breast Thickness(cm)	-0,001	0,000	-0,851	-31,090	0,000
2	(Constant)	-0,002	0,001	-	-2,043	0,042
	Breast Thickness(cm)	-0,001	0,000	-0,860	-53,185	0,000
	X-ray spectra (kV)	0,001	0,000	0,424	26,218	0,000
3	(Constant)	***-0,003***	0,001	-	-6,044	0,000
	Breast Thickness(cm)	***-0,001***	0,000	-0,873	-	0,000
	X-ray spectra (kV)	***0,001***	0,000	0,411	49,194	0,000
	Glandular_Adipose	***4,1E-5***	0,000	0,266	31,848	0,000

Here, the standardized or beta coefficient is the estimate generated from a regression analysis that have been standardized so that the variances of independent and dependent variables are 1 [43]. Therefore, standardized coefficients implies, how many standard deviations a dependent variable will change for any standard deviation change of the predictor variable. Standardization process of the independent variable is the step followed to satisfy the question of which of the independent variables have a greater effect on the dependent variable in a multiple regression analysis, when the variables are measured in different units of measurement as in our study. As to the un-standard regression beta coefficient, it indicates the average change in the dependent variable associated with a 1 unit change in the dependent variable, statistically controlling for the other independent variables. Besides, since the significance value of each independent variable is less than 0,05, ($p << 0{,}05$), three of the parameters are included in the model prediction equation. Finally, considering un-standard beta coefficients and significance value, the equation expressing the relation between three aforementioned independent variables and the dependent variable (dose) is stated as given in equation 1. In order to address the relative importance of each independent variable, the normalized values of the variables are calculated and standardized coefficients are determined accordingly. The table indicates that the relative significance of independent variables are glandular adipose, x-ray spectra and breast thickness respectively.

$$\text{dose} = (0{,}00004) * \text{GlandularAdipose} + (0{,}001 * \text{XraySpectra}) - (0{,}001 * \text{BreastThickness}) - 0{,}003 \quad \text{Eq. 1.}$$

Using the equation above, the predicted dose calculations and real system response dose values are compared. The scatterplot of measured and predicted dose is given in figure 7.

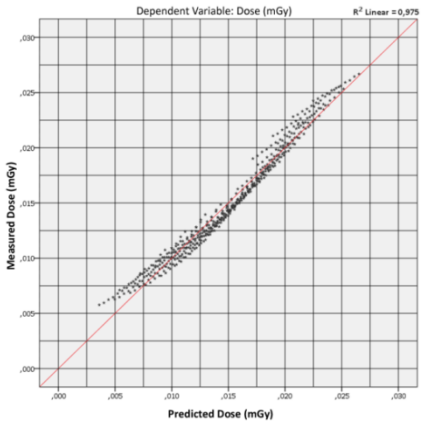

Fig. 7. Scattered measured and predicted dose value plot

4. Results and discussion

Monte Carlo techniques were used to calculate mean glandular dose values. Obtained mean glandular dose amounts reported for breast thicknesses from 2 to 12 cm by 1 cm increments. Our MLRA and ANN results underlined that, glandular adipose, breast thickness and X-ray Spectra are significant parameters affecting the absorbed dose amount in breast tissue. In this research, an experimental study employing a linear and nonlinear approach, multiple linear regression analysis and artificial neural network, is studied in order to predict the mean glandular dose in the breast tissue. The performance of both approach addresses the dose prediction problem with a quite satisfactory modeling

performance. The performance of each method is presented considering various evaluation parameters. For the artificial intelligence method, the model using TrainLM with 10 neurons in the hidden layer outperformed compared to the other models. As to the linear approach, the equation calculated as, $dose = (0{,}00004) * GlandularAdipose + (0{,}001 * XraySpectra) - (0{,}001 * BreastThickness) - 0{,}003$
satisfies the highest R2 coefficient of determination value. The neural network generated reasonable predictions of the maintenance dose (r^2 = 0.999). The results of the multiple linear regression model were similar (r^2 = 0.978).

Former literature studies also underlined the performance of both approach while predicting the glandular dose. In a study, with 63 subjects, the best results were achieved with ANN approach where correlation factor between neural network outputs and targets was r=0,845 [14]. In another study, MLRA showed that many of the instrument parameters like breast compression thickness, radiological thickness, radiation dose, compression force for acquiring the screening mammograms and image pixel intensity statistics of the imaged breasts were strong predictors of the observed threshold values (model R^2=0.93) and %density (R^2=0.84) [13]. In a recent study, neural network (r=0,823) and linear regression models (r=0,8) were used to compare the performance of each approach. The results were also quite similar considering the r values [44]. Various investigations have verified that prediction methods such as ANN have a significant potential to successfully assistance not only in estimation of mean glandular dose but also interpretation and diagnostic decisions in mammography examinations [45-47]. In this study, MCNPX Monte Carlo code techniques were used to calculate the mean glandular dose values. Validation of Monte Carlo results were compared with the results of previous investigations in literature. The calculated mean glandular dose amounts also match with previous similar results [48-50]. Application of a linear, MLRA, and a nonlinear, ANN, approach to predict the MCNPX results is promising with its remarkable results.

Small calcifications and occurrences has certainly importance and risk factor in breast tissue. Since, it is almost unfeasible to detect the exact dose amount by using detectors even in micro points of breast tissue, predictive model approaches are therefore valuable studies used to detect the absorbed dose. Thus, our research could be handled as a tool to be used to simulate radiological experiments, applications in medical physics and radiation physics research fields.

5. Conclusions

Mammography being an x-ray based breast imaging process uses radiological method as a non-invasive way for the diagnosis of breast diseases common among woman subjects. Since early diagnose of the abnormalities, mammography imaging is a valuable process in the early recognition of abnormalities in breast construction. Besides, breast dosimetry is another parameter in terms of subject radiation safety and evaluation of potential risks from medical radiation. In this research, we first aimed to put forward a mathematical model benefitting from the capabilities of MCNPX code for calculations of MGD in a mathematical breast phantom during mammography screening. MGD values were investigated by using MCNPX (version 2.4.0) Monte Carlo code.

A mathematical breast phantom has been modeled in an average shape by defining the dimensions x, y and z directions. Following Monte Carlo calculations process, multiple linear regression analysis and artificial neural network approaches were employed in order to compare their performances in terms of the absorbed dose in tissue prediction abilities. The overall performance of each method was compared considering Mean Absolute Error,

Mean Absolute Percentage Error, Root Mean Square Error, Normalized Root Mean Square Error and R-square coefficient of determination indices. The results highlighted outstanding performance of each method. In addition, promising performance of each method pointed out that MGD values are strongly correlated with three independent variables, breast thickness, X-ray spectra and glandular-adipose rate. It can be concluded that, present investigation would be very useful for similar future investigations and for scientific community.

References

[1] J. Boone, Radiology **213**, 23 (1999).

[2] L. Stanton, T. Villafana, J. Day, D. Lightfoot, Radiology **150**, 577 (1984).

[3] D. Dance, C. Skinner, K. Young, J. Beckett, C. Kotre, Phys. Med. Biol. **45**, 3225 (2000).

[4] R. Klein, H. Aichinger, J. Dierker, J.T. Jansen, S. Joite-Barfu, M. Sabel, R. Schulz-Wendtland, J. Zoetelief,
Phys.Med.Biol. **42**, 651 (1997).

[5] M. Baptista, S. Di Maria, N. Oliveira, N. Matela, L. Janeiro, P. Almeida, et al. Radiat Phys Chem.**104,** 158 (2014).

[6] I. Sechopoulos, S. Suryanarayanan, S. Vedantham, C.J. D'Orsi, A. Karellas, Radiology. **246**(2), 434 (2008).

[7] I. Sechopoulos, S. Suryanarayanan, S. Vedantham, C. D'Orsi, A. Karellas, Med Phys. **34**(1), 221 (2007).

[8] D.R. Dance, Phys Med Biol. **35**(9), 1211 (1990).

[9] K. Nigapruke, P. Puwanich, N. Phaisangittisakul, W. Youngdee, J. Radiat. Res. **51**, 441 (2010).

[10] E. Tzamicha, A. Dimitriadis, H. Gonis, E. Georgiou, V. Tsapaki, N. Yakoumakis, E. Yakoumakis, Physica Medica:
European Journal of Medical Physics. **32**(3), 326 (2016). http://dx.doi.org/10.1016/j.ejmp.2016.07.224

[11] C. Onal, G. Arslan, C. Parlak, S. Sonmez, Jpn J Radiol. **23**, 224 (2014).

[12] J. Baek, B. Kang, S. Kim, H. Lee, World J Surg Oncol. **15**, 38 (2017).

[13] W. Lee-Jane, T. Nishino, T. Khamapirad, J. Grady, M. Leonar, D. Brunder, Phys Med Biol. **52**(16): 4905 (2007).

[14] D. Ceke, S. Kunosic, M. Kopric, L. Lincender, Acta Inform Med. **17**(4), 194 (2009)

[15] S. Kunosic, An Analysis of Application of Mean Glandular Dose and Factors on Which It Depends to Patients of
Various Age Groups. Mammography - Recent Advances. 2012;7-17. DOI: 10.5772/31790

[16] S. Goto, Y. Azuma, T. Sumimoto, S. Eiho, Med Imag Tech. **21**(5), 369 (2003)

[17] RSICC Computer Code Collection. MCNPX User's manual Version 2.4.0. Monte Carlo N-Particle Transport Code
System for Multiple and High Energy Applications (2002).

[18] H.O. Tekin, MCNP-X Monte Carlo Code Application for Mass Attenuation Coefficients of Concrete at Different Energies by Modeling 3 × 3 Inch NaI(Tl) Detector and Comparison with XCOM and Monte Carlo Data. Sci Technol Nucl Ins. 2016; http://dx.doi.org/10.1155/2016/6547318.

[19] I Akkurt, H.O. Tekin, A. Mesbahi, Acta Phys Pol A. **128**(2-B), 332 (2015) doi:10.12693/APhysPolA.128.B-332.

[20] H.O. Tekin, U. Kara, Journal of Communication and Computer. (13), 32 (2016) doi:10.17265/1548-7709/2016.01.005

[21] H.O. Tekin, T. Manici, C. Ekmekci, Investigation of Backscattered Dose in a Computerized Tomography (CT) Facility during Abdominal CT Scan by Considering Clinical Measurements and Application of Monte Carlo Method. J Health Sci. 2016; 131-134. doi: 10.17265/2328-7136/2016.03.004.

[22] H.O. Tekin, V.P. Singh, T. Manici, Appl. Radiat. Isot. **121**, 122 (2017); doi:http://dx.doi.org/10.1016/j.apradiso.2016.12.040
[23] G. Verdú, A. Leön, J.I. Villaescusa, M.D. Salas, M. D. Cuevas, F. Bueno, J. Nucl. Sci. Technol. **37**(1) 875 (2000) DOI:10.1080/00223131.2000.10875015
[24] G. R Hammerstein, D. W. Miller, D. R. White, M. E. Masterson, H. Q. Woodard, J. S. Laughlin, Radiology. **130**(2), 485 (1979). doi: 10.1148/130.2.485.
[25] L. Gholamkar., A. A. Mowlavi, M. Sadeghi, M. Athari Iran J Radiol. **13**(4) doi: 10.5812/iranjradiol.36484
[26] H. Zhao, F. Magoul_es, Renew Sustain Energy Rev **16,** 3586 (2012).
[27] F. Khademi, K. Behfarnia, Iran Univ. Sci. Technol.; **6**(3), 423 (2016).
[28] S.I.V. Sousa, F.G. Martins, M.C.M. Alvim-Ferraz, M.C. Pereira, Environ. Model. Softw. **22,** 97 (2007).
[29] J.C.M. Pires, F.G. Martins, S.I.V. Sousa, M.C.M. Alvim-Ferraz, M.C. Pereira, Environ. Model. Softw. **23**, 50 (2008).
[30] I. Ceylan, Drying Technol **26**(12), 1469 (2008).
[31] A. Canakci, S. Ozsahin, T. Varol, Powder Technol **228**, 26 (2012).
[32] A.M. Hassan, A. Alrashdan, M.T. Hayajneh, A.T. Mayyas, J Mater Process Technol **209**, 894 (2009).
[33] S. Tiryaki, S. Ozsahin, I. Yildirim, Int. J. Adhes. Adhes. **55**, 29 (2014).
[34] H.R. Maier, G.C. Dandy, Environ Model Softw.15(1), 101 (2000).
[35] W.S. Sarle, Stopped training and other remedies for overfitting. Paper presented at the Proceedings of the 27th Symposium on the Interface. 1995.
[36] G. Zhang, B. Eddy Patuwo, M.Y. Hu,. Int J Forecasting. **14**, 35 (1998).
[37] R. Fletcher, Practical Methods of Optimization, John Wiley & Sons, 2000.
[38] U. Atici. Prediction of Concrete Compressive Strength by Evolutionary Artificial Neural Networks. Expert Syst Appl. 2011;38:9609–9618.
[39] A. A. Suratgar, M. B. Tavakoli, A. Hoseinabadi, World Acad Sci Eng Technol. **6**, 46 (2005)
[40] H. Akbarpour, M. Mohajeri, M. Moradi, Comput Mater Sci. **79**, 75 (2013).
[41] G. Zhang, B.E. Patuwo, M.Y. Hu, Int J Forecast **14**, 35 (1998).
[42] S. Azadi, A. Jashni, Iran. Waste Manage. **48,** 14 (2016).
[43] D.Larry, L.David, E. Paula, Understanding regression analysis, Sage Publications. ISBN 0-8039-2758-4, 1986;31-32.
[44] I. Solomon, N. Maharshak, G. Chechik, Isr Med Assoc J. **6**(12), 732 (2004).
[45] A. Turgay, C. Qiushi, S. Elizabeth, Artificial Neural Networks in Mammography Interpretation and Diagnostic Decision Making. Comput Math Methods Med. 2013; doi:10.1155/2013/832509
[46] Y. Wu, M.L. Giger, K. Doi, C.J. Vyborny, R.A. Schmidt, C. E. Metz, Radiology. **187**(1), 81 (1993).
[47] C. Markopouloas, E. Kouskos, K. Koufopoulos, V. Kyriakou, J. Gogas, Eur J Radiol **39**(1), 60 (2001).
[48] A. Bozkurt, H. Acun, G. Kemikler, Jpn J Radiol **31**, 24 (2013).
[49] A. Ezzati, A. Pashazadeh, M. Studenski, Monte Carlo Simulation of the RBE of I-131 Radiation Using DNA Damage as Biomarker. Australas Phys Eng Sci Med. 2017;1-6. DOI: 10.1007/s13246-017-0544-4.
[50] R. Ahangari, H. Afarideh, Australas Phys Eng Sci Med. **34,** 467 (2011).